

Contents lists available at ScienceDirect

### International Journal of Applied Earth Observations and Geoinformation

journal homepage: www.elsevier.com/locate/jag





## The potential of active and passive remote sensing to detect frequent harvesting of alfalfa

Yuting Zhou <sup>a,\*</sup>, K. Colton Flynn <sup>b</sup>, Prasanna H. Gowda <sup>c</sup>, Pradeep Wagle <sup>d</sup>, Shengfang Ma <sup>e</sup>, Vijaya G. Kakani <sup>f</sup>, Jean L. Steiner <sup>g</sup>

- <sup>a</sup> Department of Geography, Oklahoma State University, Stillwater, OK 74078, USA
- <sup>b</sup> USDA-ARS, Grassland Soil and Water Research Laboratory, Temple, TX 76502, USA
- <sup>c</sup> USDA-ARS, Southeast Area, Stoneville, MS 38776, USA
- <sup>d</sup> USDA-ARS, Grazinglands Research Laboratory, El Reno, OK 73036, USA
- e Department of Computer Science, Oklahoma State University, Stillwater, OK 74078, USA
- f Department of Plant and Soil Sciences, Oklahoma State University, Stillwater, OK 74078, USA
- g Agronomy Department (Adjunct), Kansas State University, Manhattan, KS 66502, USA

#### ARTICLE INFO

# Keywords: Optical remote sensing Radar Data fusion Spatial and temporal resolutions Crop monitoring

#### ABSTRACT

Alfalfa (Medicago sativa L.), referred to as the "Queen of Forages" because of its importance among forage crops, provides high quality forage for the livestock industry. The timing and frequency of alfalfa hay harvesting have implications on its quality and quantity. With ever-increasing capability, it is possible to use satellite remote sensing data to monitor alfalfa harvests. This study investigated the potential of using satellite remote sensing to capture frequent harvesting events on an alfalfa field in central Oklahoma. Both passive remote sensing data, namely Moderate Resolution Imaging Spectroradiometer (MODIS), Landsat-7 and -8, Sentinel-2, Harmonized Landsat and Sentinel-2 (HLS), and active remote sensing data, namely Sentinel-1, were included. Our results indicate that good quality optical remote sensing datasets (i.e., cloud and cloud shadow free) with both fine spatial (<100 m) and high temporal (effective observation at 8-day intervals or better) resolutions are necessary to detect frequent alfalfa harvesting events, challenged by possible adverse weather conditions and quick regrowth of vegetation after harvest. Landsat (7 and 8) and Sentinel-2 were more sensitive to changes in vegetation indices after harvest than MODIS due to their higher spatial resolutions, which helped avoid the mixed pixel issue in MODIS caused by its coarser spatial resolution (~500 m). Combining Landsat (7 and 8) with Sentinel-2 imageries through linear regression between the Normalized Difference Vegetation Index (NDVI) values, up to one week apart, increased the accuracy of detecting frequent alfalfa harvesting events. The responses of HLS to alfalfa harvesting events were similar with fused Landsat and Sentinel-2 data using their linear relationship of NDVI values. However, the high noise level in the HLS data needs to be minimized before it can be used to detect alfalfa harvests at the regional scale. In most cases, both Sentinel-1 radar backscatter coefficients (vertical transmit and vertical receive, VV + vertical transmit and horizontal receive, VH) and interferometric coherence from Sentinel-1 Simple Look Complex (SLC) data were decreased by harvesting events in small incident angle observations (34.31°). No consistent relationships existed between backscatter or coherence and alfalfa harvests in larger incident angle observations ( $45.11^{\circ}$ ). Future studies should focus on small incident angle observations instead of processing all of the radar data, which has big data volume and is time-consuming. Overall, active radar has the potential to detect alfalfa harvesting events. However, it is visually less intuitive than optical data with incident angles, quantity harvested, and soil moisture being the compounding factors. This study illustrates that combining multiple optical sensors with a fine spatial resolution (e.g., Landsat-7, 8, and Sentinel-2) and/or fusing radar with optical remote sensing to increase the temporal resolution are promising approaches to detect frequent alfalfa harvesting events and other hay harvesting activities.

E-mail address: yuting.zhou@okstate.edu (Y. Zhou).

<sup>\*</sup> Corresponding author.

#### 1. Introduction

Alfalfa (*Medicago sativa* L.) has been cultivated as an important forage crop in as many as 80 countries around the world and is the most intensively produced (52.6 M tons in 2018) perennial forage crop in the United States (U.S. Department of Agriculture – National Agricultural Statistics Services 2019). Alfalfa provides high quality protein, vitamins, and energy for livestock, including dairy cattle in the Southern Great Plains (SGP) of the U.S. (Burris 2001; Butler et al., 2012; Caddel et al., 2001). Information about the harvested area of alfalfa is thus important for the livestock industry as an indication of forage availability. The livestock industry usually depends on statistical data (e.g., survey data from the U.S. Department of Agriculture – National Agricultural Statistics Service, USDA-NASS) to obtain harvested alfalfa acreage and yield data, which has a coarse spatial resolution (county-level or coarser) and is usually available one year after the survey (e.g., USDA-NASS releases annual agricultural statistics for the previous year in the current year).

Alfalfa is generally on a four-year rotation as the legume fixes nitrogen well for rotational crops, such as corn, and because young stands of alfalfa vield more than old stands (Noland et al., 2018; Undersander et al., 2011). Common management practices account for proper irrigation, weed and pest controls via chemical application, disease/insect management, and fertilization (Undersander et al., 2011). When managed properly, an alfalfa field can be harvested several times during the growing season depending on varying climate and soil conditions (Caddel et al., et al., et al., 2001). Due to large variability in climate in the SGP, alfalfa growth is highly variable as regrowth following harvest depends on the timing of harvesting during the growing season (growth stage) and precipitation (Zhou et al., 2017b). To detect the frequent and variable alfalfa harvests at a large scale, it is necessary to utilize high temporal resolution remote sensing data. Additionally, the spatial resolution of the satellite data also needs to account for varying sizes of alfalfa fields (with width and length range from several hundred meters to 1.6 km in the SGP). For instance, the Moderate Resolution Imaging Spectroradiometer (MODIS) provides daily surface reflectance products, but its spatial resolution (~500 m) might be too coarse to monitor alfalfa harvesting in small fields because of the occurrence of mixed pixels. The large, often mixed, pixels of MODIS have been a challenge for many agriculture field studies in the past (Flynn et al., 2020; Zhou et al., 2019). Compared to the coarse spatial resolution of MODIS, Landsat (7 and 8) has a finer spatial resolution (30 m). However, it has a lower temporal resolution (16 days). The adverse weather condition (e.g., cloud and cloud shadow) during Landsat overpass further reduces its availability. Thus, the use of Landsat data alone may not be sufficient for detecting these short-term harvesting events. Sentinel-2 has spectral bands similar to Landsat-8 and has a temporal resolution of five days. With its higher temporal resolution, it may better detect the frequent alfalfa harvesting events. Since both Sentinel-2 and Landsat-8 have similar band configurations, they can be merged to further increase the temporal resolution (Claverie et al., 2018; Griffiths et al., 2019). However, all of these are optical sensors and are susceptible to adverse weather conditions.

Unlike optical sensors, active radar sensors are not sensitive to weather conditions. Thus, short-term land surface changes can be detected using high temporal resolution radar. Radar remote sensing methods have been applied to agriculture to predict leaf area index (Hosseini et al., 2015), soil moisture (Zhu et al., 2019), phenology (McNairn et al., 2018), and growth conditions (Mandal et al., 2020) using many different polarizations and bands (Bégué et al., 2018). For instance, Sentinel-1 is a satellite mission with an active radar sensor and has been used to monitor mowing events on grasslands (Tamm et al., 2016).

With an ever-increasing volume of remote sensing data and higher spatial, temporal, and spectral resolutions, we hypothesize that it is possible to detect the frequent harvesting of alfalfa using remote sensing. To test the potential of using satellite remote sensing to detect

frequent alfalfa harvesting events, this study used multiple remote sensing datasets, namely MODIS, Landsat-7 and -8, and Sentinel-1 and -2 over an alfalfa field in central Oklahoma during a two-year study period (2016–2017). Multiple data fusion methods including simple linear regression and principle driven fusion approach were included. The sensitivity of these datasets to alfalfa harvesting events was also evaluated. This study, using both active and passive remote sensing data to detect the frequent harvesting of alfalfa, can provide a proof of concept for new regional monitoring technologies for alfalfa harvesting.

#### 2. Study site and data retrieval

#### 2.1. Site description

The study site, an alfalfa field, is located at the USDA-Agricultural Research Service (USDA-ARS), Grazinglands Research Laboratory (GRL) in El Reno, Oklahoma (Fig. 1). The field (triangle in Fig. 1) was planted with alfalfa (Cimarron VL400) in fall 2012 and managed under rain-fed condition. The major soil types in the field are Dale silt loam and Brewer silty clay loam according to data from the Soil Survey Geographic Database (https://websoilsurvey.sc.egov.usda.gov/App/HomePage.htm).

#### 2.2. Climate data

The Oklahoma Mesonet El Reno station, which provides quality-controlled measurements of major meteorological variables (McPherson et al., 2007), is 3 km to the south of the study area. Precipitation was more evenly distributed in 2016 than in 2017 (Fig. 2). However, the total precipitation was less in 2016 (63.14 cm) compared to 2017 (110.92 cm). There was little rain during the early growing season in 2016 while a dry spell existed in October and November of 2017.

#### 2.3. Harvesting record for the alfalfa field

The field was harvested for hay multiple times each year depending on weather conditions and forage availability. Table S1 presents the harvest dates and forage yields for each harvesting event during the study period.

#### 2.4. Satellite data

For inter-comparison, multiple satellite remote sensing datasets including both active and passive remote sensing were incorporated. Sentinel-1 is a satellite platform with an active radar. Sentinel-2, Landsat-7 and -8, and MODIS are satellite platforms with passive optical sensors. Table 1 provides a brief summary of satellite datasets used. The Harmonized Landsat and Sentinel-2 (HLS), which fuses Landsat-8 and Sentinel-2, was also included. More information about each dataset is described in the supplementary material, and employed data analysis (Fig. 3) is described in the following sections.

#### 3. Data analysis

#### 3.1. Quality control of optical data

For each of the three optical remote sensing datasets (e.g. MODIS, Landsat-7 and -8, Sentinel-2), their respective quality assessment information was used to exclude image artifacts caused by cloud, cloud shadow, and aerosols. Specifically, all MODIS data that did not pass the quality control were excluded for further analyses based on the following criteria: cloud state flag indicates cloudy or mixed, or cloud shadow existence, or aerosol quantity flag shows high, or cirrus-detected flag is average or high. Only clear pixels in Landsat-7 and -8 data, indicated by the pixel quality band, were included. Similar quality control processes were implemented for the Sentinel-2 and HLS datasets

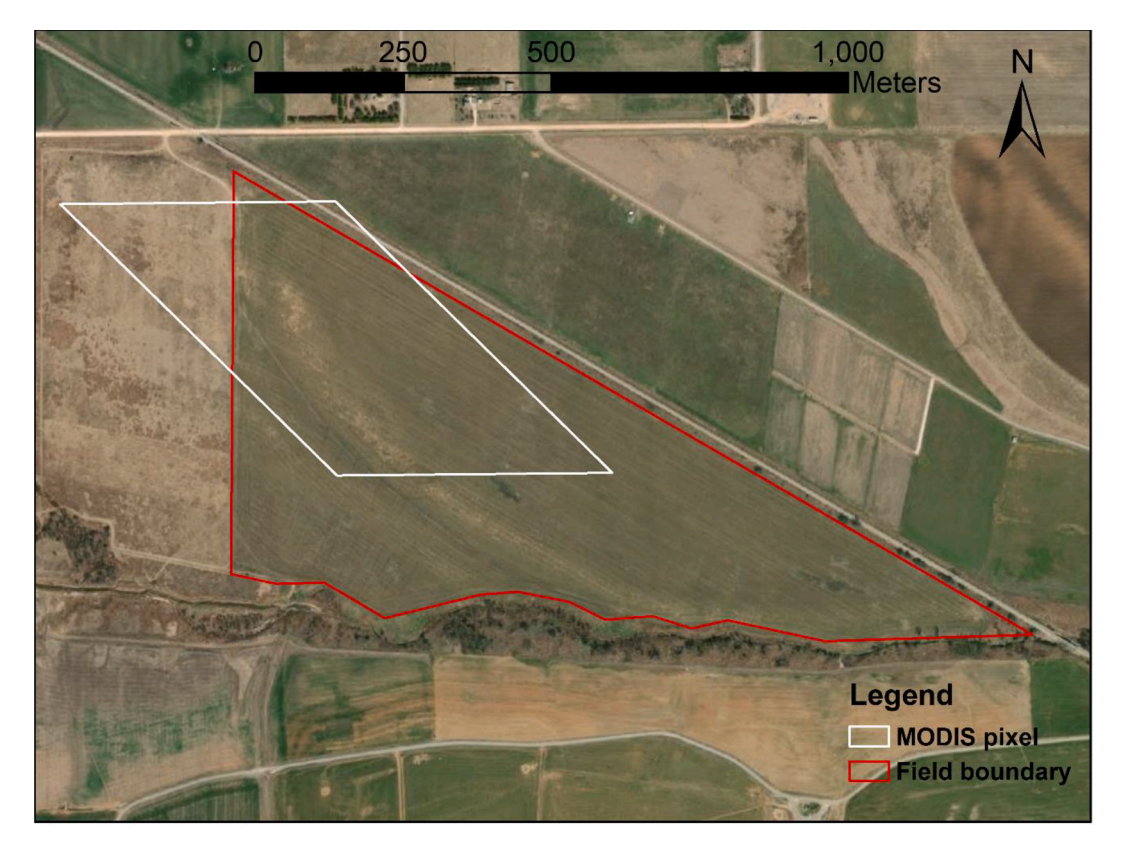


Fig. 1. Study site overlapping with the Moderate Resolution Imaging Spectroradiometer (MODIS) pixel.

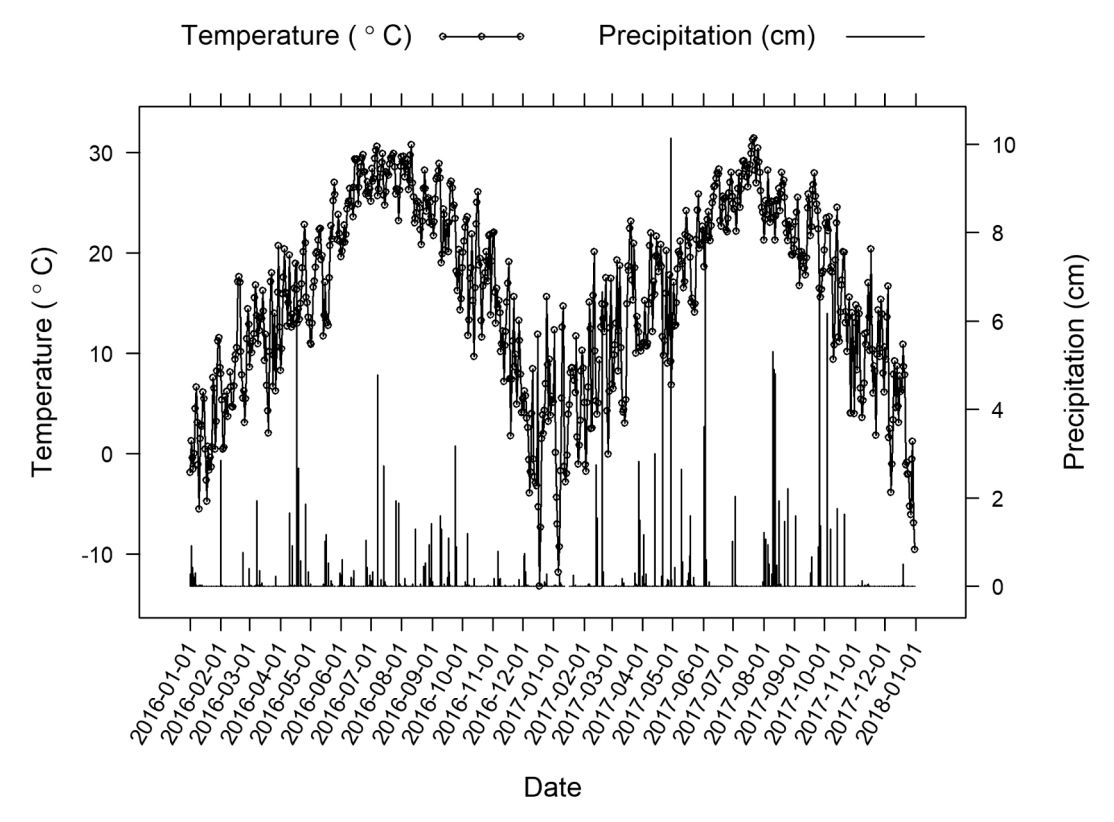


Fig. 2. Daily average air temperature and daily precipitation for 2016–2017 from the Oklahoma Mesonet El Reno station.

where cloud, cloud shadow, cirrus, and high aerosol observations were excluded using the SC map (Müller-Wilm et al., 2016) and the quality assessment layer in Sentinel-2 and HLS, respectively. Further analysis

only included those dates with the ratio of good quality pixels more than 50%. This strict quality control step helps reduce the noise when calculating vegetation indices (VIs) and correlating them with

**Table 1**A brief summary of satellite datasets used in this study.

Satellite	Product type	Spatial resolution	Temporal resolution	Number of images
Sentinel-	Ground Range	20 m	12 days	91
1A	Detected			
Sentinel-	Top-Of-Atmosphere	10 m	10 days	41
2A	Reflectance			
Sentinel-	Top-Of-Atmosphere	10 m	10 days	11
2B	Reflectance			
Landsat 7	Surface Reflectance	30 m	16 days	39
Landsat 8	Surface Reflectance	30 m	16 days	32
MODIS	Surface Reflectance	500 m	8 days	92

harvesting events.

#### 3.2. Vegetation indices (VIs) calculation

Two widely used VIs, namely Normalized Difference Vegetation Index (NDVI) and Enhanced Vegetation Index (EVI), were calculated from the quality controlled surface reflectance from respective optical remote sensing datasets in blue ( $\rho_{blue}$ ), red ( $\rho_{red}$ ), and NIR ( $\rho_{nir}$ ) bands (Eqs. (1) and (2)) (Huete et al., 2002; Tucker 1979). These VIs are commonly used in remote sensing methods to represent biomass (Bartsch et al., 2020; Weiss et al., 2020; Yang et al., 2018). The NIR bands used in calculating VIs for MODIS and Sentinel-2 were 841–876 nm and 785–900 nm, respectively.

$$NDVI = \frac{\rho_{nir} - \rho_{red}}{\rho_{\perp} + \rho_{\perp}} \tag{1}$$

$$EVI = 2.5 \times \frac{\rho_{nir} - \rho_{red}}{\rho_{nir} + 6.0 \times \rho_{red} - 7.5 \times \rho_{blue} + 1}$$
 (2)

After VIs were computed, the mean VIs for the alfalfa field was extracted to represent the average condition of the field. Moreover, for depiction purposes, shortwave infrared (SWIR), NIR, and red bands were used to develop false color composite images for harvesting events with

large and small quantities harvested (i.e., large and small harvests).

## 3.3. Fusing Landsat and Sentinel-2 data with statistical transformation function

The HLS dataset includes both Landsat-8 and Sentinel-2 data. However, it does not include Landsat-7 data, and the Sentinel-2 cloud masking omission is a known issue with HLS (Claverie et al., 2018). To further improve the temporal resolution of the fine spatial resolution optical remote sensing data, we combined VIs derived from Landsat (7 and 8) and Sentinel-2. For this purpose, we compared Landsat and Sentinel-2 based NDVI values, which were observed up to one week apart. A simple linear regression was performed for those observations and the slope of the regression was applied to calibrate Sentinel-2 based NDVI and EVI to Landsat observations (i.e., Landsat based VIs are independent variables). The fused Landsat and Sentinel-2 data were then used as a new dataset to detect frequent alfalfa harvesting events.

#### 3.4. Sentinel-1 backscatter and interferometric coherence

Our study area was covered by two orbits (34 and 107) but with different incident angles by Sentinel-1. Orbit 34 has an incident angle of  $34.31^{\circ}$ , while orbit 107 has an incident angle of  $45.11^{\circ}$  for the study site. The Sentinel-1 Ground Range Detected (GRD) products were used to calculate the geocoded backscatter coefficient ( $\sigma^{\circ}$ ), and the Single Look Complex (SLC) data was used to obtain the interferometric coherence using the Sentinel Application Platform (SNAP). Details of data processing steps can be found in the supplementary material.

Time-series of VV and VH backscatter coefficient and coherence for the entire alfalfa field were extracted to show their sensitivity to different harvest yields. To examine the impact of the incident angle in determining the response of backscatter and coherence to alfalfa harvest, we analyzed the data for the two orbits separately.

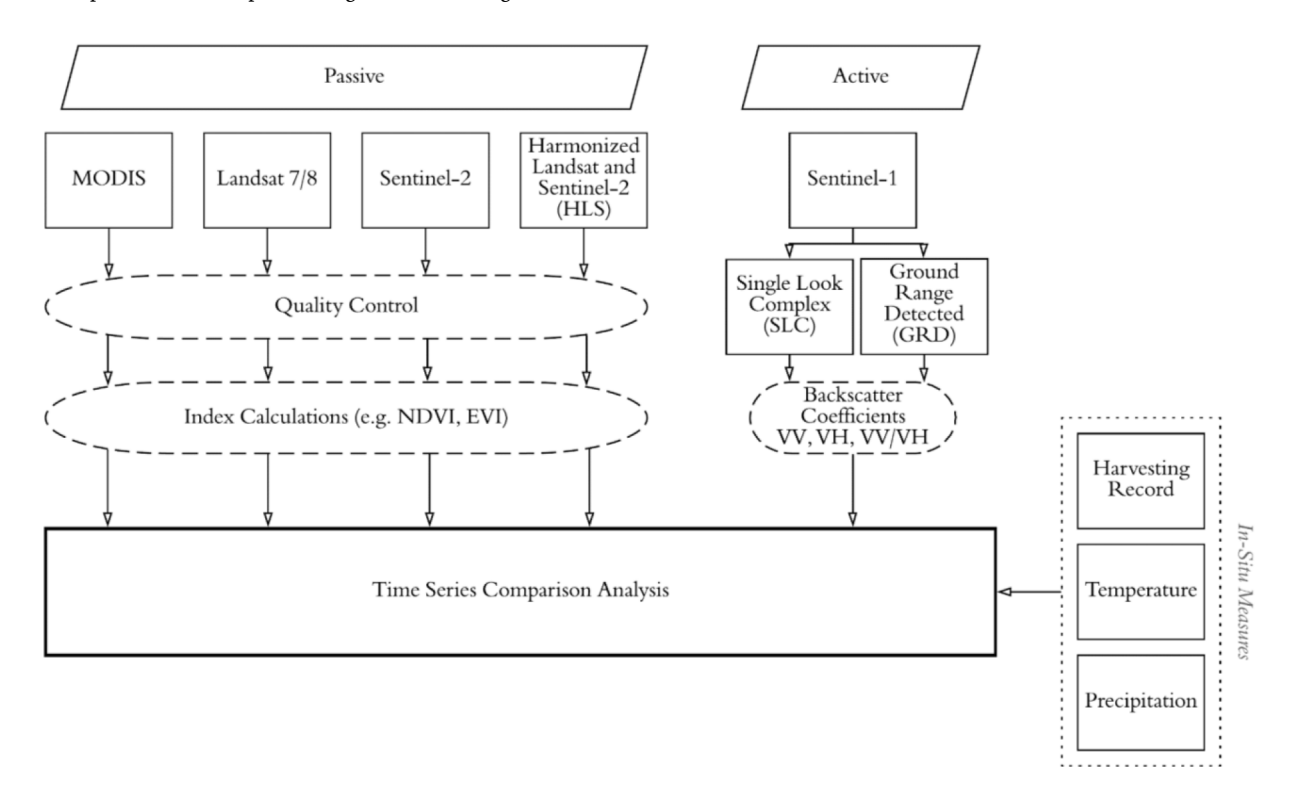


Fig. 3. Methodological flowchart of the study. NDVI: Normalized Difference Vegetation Index; EVI: Enhanced Vegetation Index; VV: vertical transmit and vertical receive; VH: vertical transmit and horizontal receive.

#### 3.5. Sensitivity analysis

Since remote sensing datasets have different temporal resolutions, sensitivity analysis was done for comparison purposes. The change rate, (present – past)/ (time difference in days), for each dataset was used to indicate its sensitivity. All optical remote sensing datasets, including MODIS, Landsat, Sentinel-2, HLS, and fused Landsat and Sentinel-2 were grouped in one group, while radar data in two orbits were treated as another group. The sensitivity analysis then utilized each of the two groups of data to understand which instance of optical/active data groupings were most sensitive to the harvesting events. The sensitivity analysis proposed here considers the duration between the revisit time of the given platform that may or may not have been hindered by clouds, affecting the temporal resolution. By using this sensitivity analysis, we are combining the platform's spectral and temporal abilities to better understand the platform's given potential in detecting frequent alfalfa harvests.

#### 4. Results

#### 4.1. VIs derived from single optical remote sensing dataset

Both NDVI and EVI were highly correlated with each other in all single optical remote sensing dataset as expected (Figs. 4–6). Their values decreased immediately following the harvesting events. However, the decrease in VIs caused by harvests did not necessarily correlate with the size of the harvesting events, especially for the largest harvest (June 7, 2017, with a forage yield of 4.41 t ha<sup>-1</sup>) in which MODIS-derived NDVI values only decreased slightly (Fig. 4). The decrease in Landsat- and Sentinel-2-derived NDVI and EVI was more closely related to the size of the harvesting events (Figs. 5 and 6 middle panels) compared to MODIS-derived VIs (Fig. 4). However, both Landsat and Sentinel-2 missed some harvesting events (e.g., Landsat and Sentinel-2 missed the harvesting events on May 18, 2016 and May 3, 2017, respectively).

The impacts of harvesting on land surface were captured in the color composite images before and after alfalfa harvesting from Landsat and Sentinel-2 (Figs. 5 and 6 top and bottom panels). Note that the differences of the field before and after harvests were much clearer in a small (Fig. 5 bottom panels) than a large harvesting event (Fig. 5 top panels), which will be explained later in Section 4.3. The timing (Fig. 6a and d) and size (Table S1) of harvesting events jointly determined the impacts of each harvest (Fig. 6b and e) on surface reflectance.

#### 4.2. VIs derived from the HLS data

The HLS data that incorporated both Landsat-8 and Sentinel-2 increased the temporal resolution of VIs (Fig. 7). HLS-derived VIs decreased significantly in response to most of the harvesting events. However, the noise level was also high in the HLS-derived VIs, which causes some abnormal values. For example, NDVI and EVI increased after harvest in August. To further examine the reasons for the high noise level in HLS, we compared the results of HLS-derived NDVI and EVI with those directly from Landsat (Fig. S1) and Sentinel-2 (Fig. S2). Possible causes for the high noise are the inclusion of both Landsat-8 Collection-1 Tier-1 and Tier-2 data (Fig. S1), Sentinel-2 cloud masking omission (Fig. S2), and Bidirectional Reflectance Distribution Function (BRDF) adjustment (see Claverie et al., 2018 for more details) in HLS data processing. The impacts of cloud masking omission were also manifested by the abrupt increases in NDVI during winter (black dashed circle in Fig. 7). These noises pose challenges to separate the drops in the signal from the true harvesting events.

#### 4.3. VIs derived from fused Landsat and Sentinel-2 data

There was a good linear relationship ( $\rm r^2=0.87$ ) between NDVI values derived from Landsat (7 and 8) and Sentinel-2 that were acquired up to one week apart (Fig. 8). The slope of the regression was  $\sim$ 1, indicating that Landsat and Sentinel-2 derived VIs can be merged to increase the temporal resolution of the data. The slope of the regression was applied to calibrate Sentinel-2 based VIs to Landsat observations.

Combining Landsat and Sentinel-2 derived VIs increased the possibility of detecting frequent alfalfa harvesting events (Fig. 9). VIs decreased significantly after each harvesting event except for the small harvest on August 9, 2017 (Table S1), which was followed by a large precipitation event (Fig. 2). Both NDVI and EVI had similar performance in detecting alfalfa harvests. The decrease in VIs was positively correlated with the size of harvesting events in general. The recovery of vegetation growth after harvest was better captured by this higher temporal resolution dataset. NDVI was already low right before the last harvest in 2017 (a small harvest). The following harvesting event thus further decreased the NDVI, which caused a distinct contrast before and after harvest than the one in a larger harvest (Fig. 5). Comparing the fused Landsat and Sentinel-2 NDVI to the HLS-derived NDVI, the former had much lower noise levels due to its strict and consistent quality control process (Section 3.1). Nevertheless, there was a very strong linear relationship between HLS-derived NDVI and fused Landsat and Sentinel-2 NDVI (Fig. S3), indicating that HLS well harmonized good quality Landsat-8 and Sentinel-2 observations.

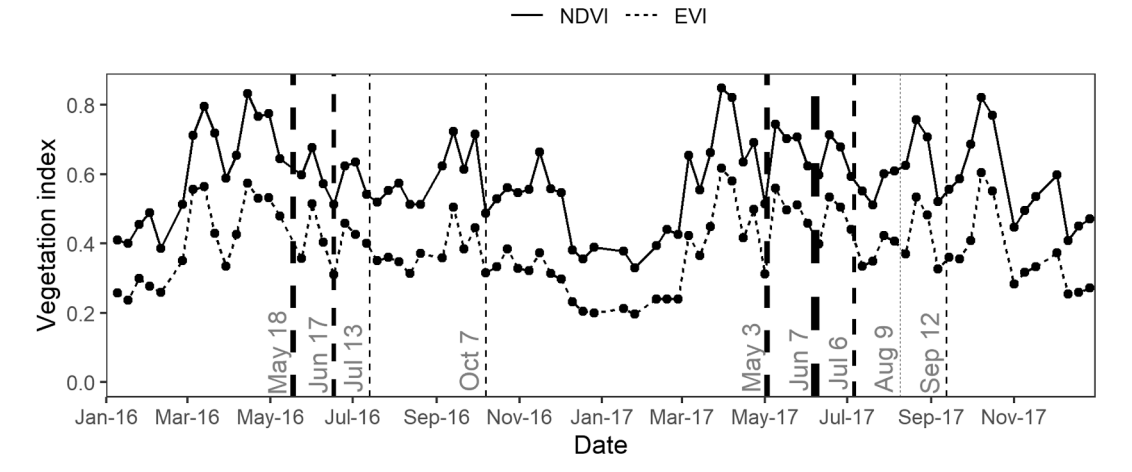


Fig. 4. Dynamics of Normalized Difference Vegetation Index (NDVI) and Enhanced Vegetation Index (EVI) from the MODIS integrated with harvesting events (dash lines, with the width of the lines indicating forage yield).

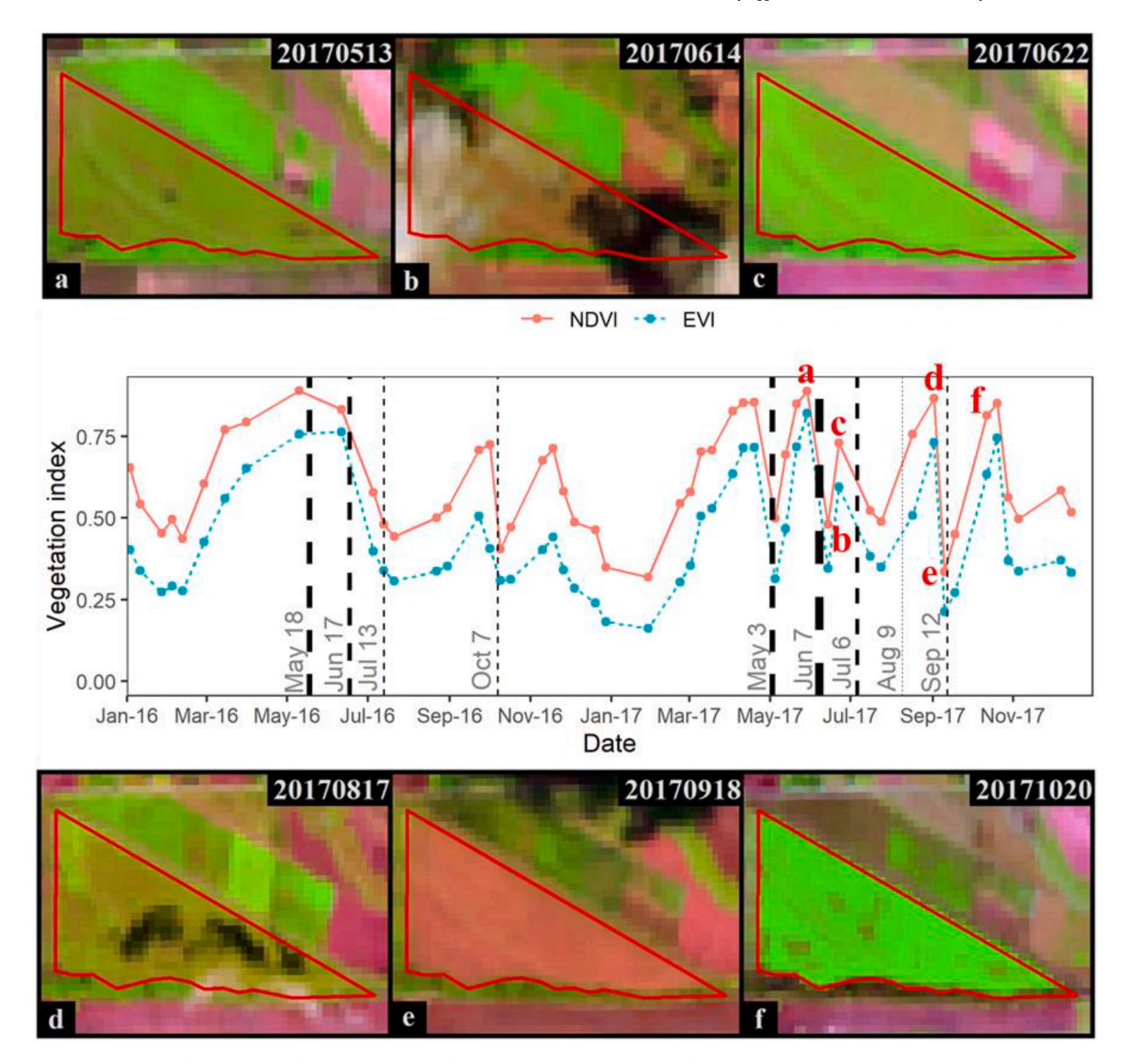


Fig. 5. Dynamics of NDVI and EVI from Landsat-7 and -8 and color composite (SWIR-2, NIR, and red) images for large and small harvesting events in 2017. (For interpretation of the references to color in this figure legend, the reader is referred to the web version of this article.)

#### 4.4. Radar backscatter from Sentinel-1

Dynamics of VV and VH backscatter coefficients from Sentinel-1 (Fig. 10 middle panel) were similar in orbit 34, which has a smaller incident angle (34.31°). In most cases, VV and VH backscatter coefficients were decreased by harvests. In addition, VV backscatter coefficients during the growing season (April-October) decreased only after harvest. The decrease in VV and VH backscatter coefficients at the end of the growing season and their fluctuations during the early spring period indicated the importance of plant phenology and soil moisture on radar backscatter. The color composite images before (Fig. 10a and d) and after (Fig. 10b and e) harvests showed the impacts of harvesting on radar backscatter. However, the contrasts between before and after harvests were not as clear as the contrasts seen in Landsat and Sentinel-2 imageries (Figs. 5 and 6). The speckle noise also increased the difficulty of the interpretation of radar images (Fig. 10 top and bottom panels).

There were no consistent relationships between VV and VH back-scatter coefficients from Sentinel-1 with alfalfa harvest in orbit 107 (Fig. 11), which has a larger incident angle  $(45.11^{\circ})$ . The dynamics of backscatter were not relevant to the size of the harvesting events. As

seen in the observations with a smaller incident angle (Fig. 10 middle panel), the backscatter decreased at the end of the growing season and fluctuated during the non-growing season for the larger incident angle observations.

#### 4.5. Interferometric coherence from Sentinel-1

Dynamics of VV and VH interferometric coherence from Sentinel-1 (Fig. 12 middle panel) were mostly similar in orbit 34, which has a smaller incident angle (34.31°). In contrast to backscatter coefficients (Fig. 11), the interferometric coherence coefficients were increased by harvesting events. However, similar to the backscatter coefficient, the background noise was high in the coherence time-series. For example, there were two evident peaks of VV and VH coherence around August of 2016 and January of 2017, which were not caused by harvesting events. The contrasts of color composite images, derived from coherence bands, between before and after harvests were not as clear as seen in Landsat and Sentinel-2 imageries (Figs. 5 and 6). As in the case of the backscatter coefficient, there were no consistent relationships between VV and VH interferometric coherence coefficient from Sentinel-1 with alfalfa

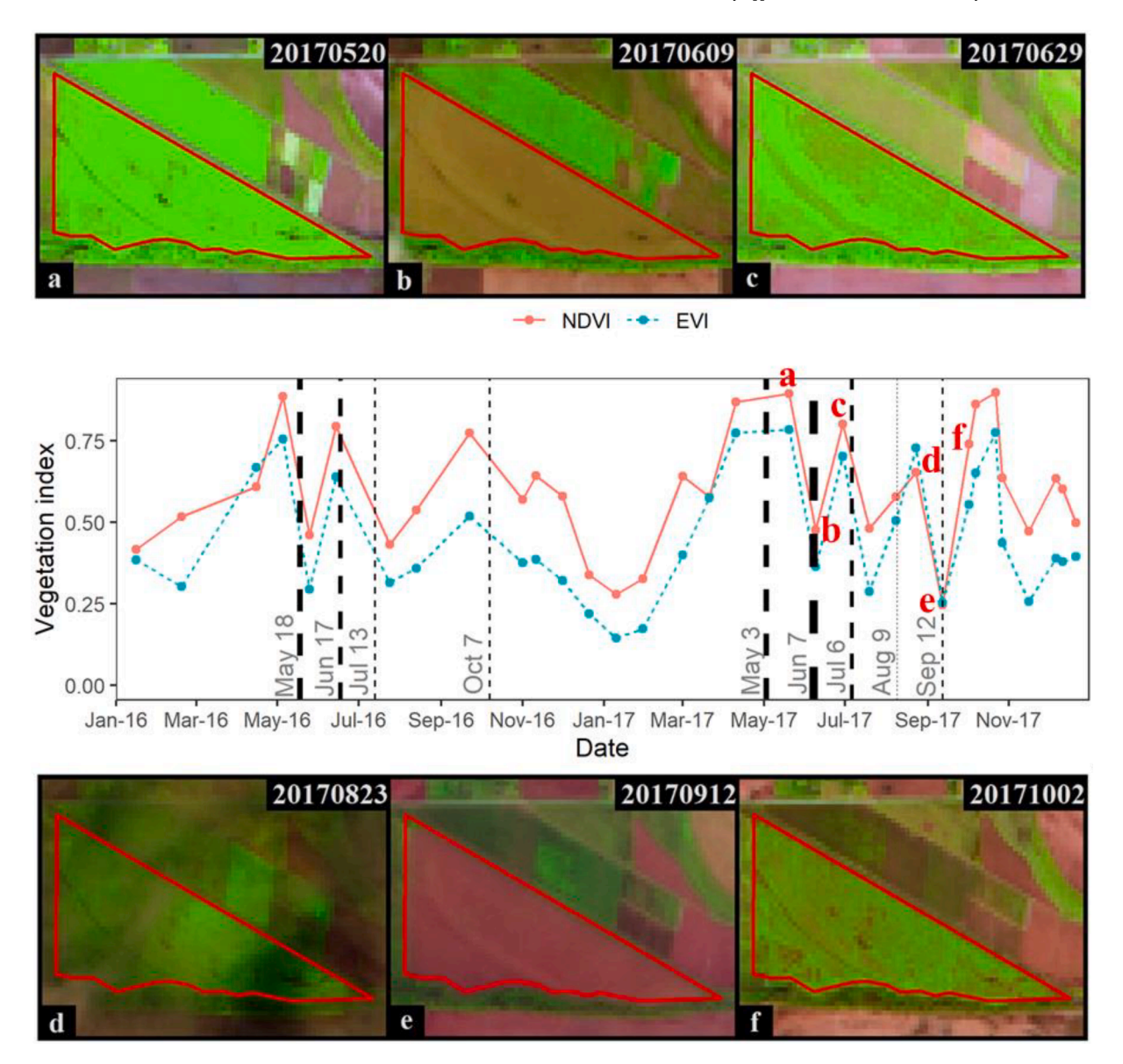


Fig. 6. Dynamics of NDVI and EVI from Sentinel-2 and color composite (Shortwave infrared (Band 11), near-infrared (Band 8), and red (Band 4)) images for large and small harvesting events in 2017. (For interpretation of the references to color in this figure legend, the reader is referred to the web version of this article.)

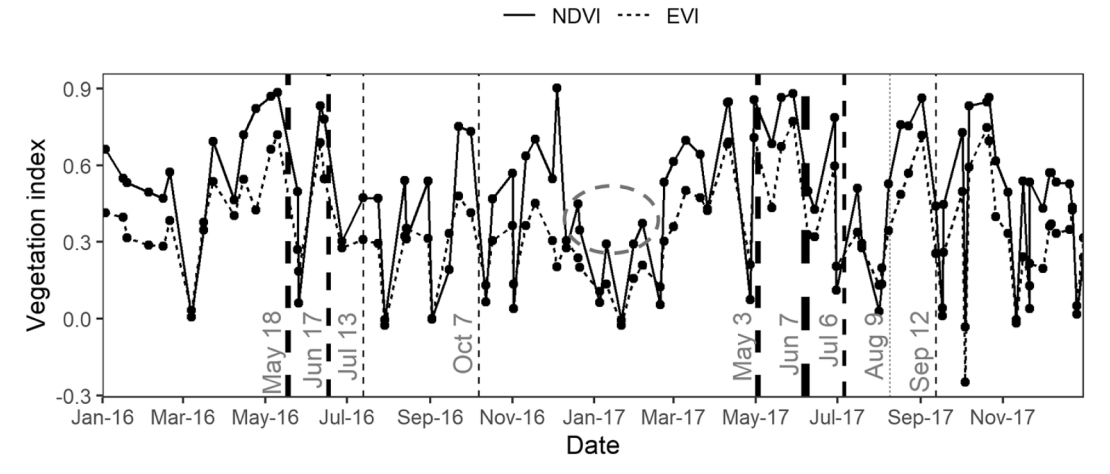


Fig. 7. Dynamics of NDVI and EVI from the HLS data. The black dashed circle indicates the impacts of cloud masking omission on vegetation indices.

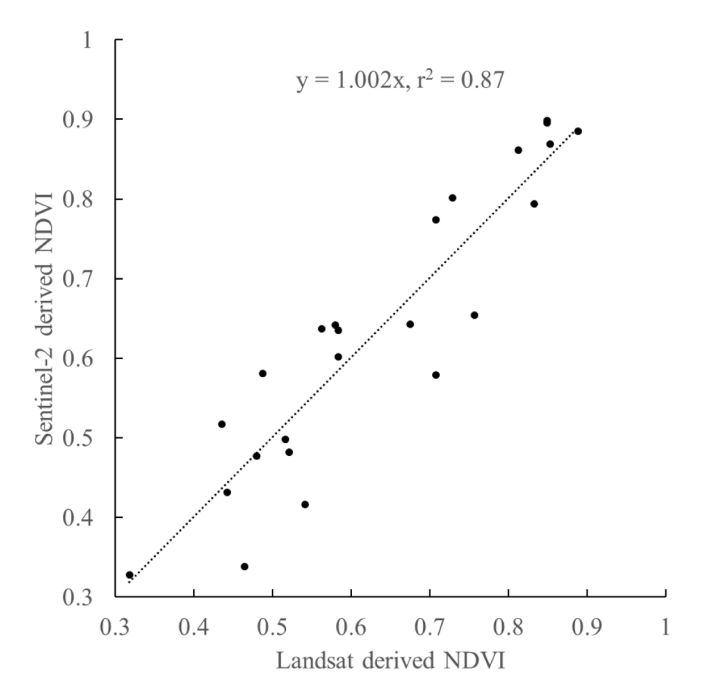


Fig. 8. Relationship between Landsat derived and Sentinel-2 derived NDVI for one week apart.

harvest in orbit 107 (Fig. S4), which has a larger incident angle (45.11°).

#### 4.6. Sensitivity of each dataset to detect different sized harvesting events

The decrease in VIs caused by harvests were larger in Landsat and Sentinel-2 (Fig. 13b and c) than in MODIS (Fig. 13a), indicating the former is spatially more sensitive than the latter in detecting alfalfa harvests. The higher spatial resolutions of Landsat and Sentinel-2 helped avoid the mixed pixel issue in MODIS caused by its coarser spatial resolution. However, MODIS can better depict all harvest events and reflect the impacts of climate on alfalfa because of its higher temporal resolution. The changes in VIs in HLS (Fig. 13d) and our fused Landsat and Sentinel-2 data (Fig. 13e) were more evident after each harvest, indicating improved detection of alfalfa harvests. However, the noise level increased in the HLS and our fused Landsat and Sentinel-2 data, especially in the former, which makes it hard to differentiate VIs decreases caused by harvesting events and noises in the dataset.

The radar backscatters were mostly decreased by harvests in smaller incident angle observations (34.31°) (Fig. 14a). There were also significant changes in backscatter during the non-growing season, probably

caused by the dynamics of soil moisture. The change in radar backscatter was not consistently correlated with the alfalfa harvests in the larger incident angle observations (45.11°) (Fig. 14b). Similar to the radar backscatters, the coherence in smaller incident angle observations (Fig. 14c) were more sensitive to harvesting events than those in the larger incident angle observations (Fig. 14d), which were largely not responsive to the harvesting events. However, as it was mentioned before, the coherence was increased by harvesting events, in contrast to backscatter (Fig. 14a). There were other factors besides harvesting that affected the dynamics of coherence. For example, the coherence values decreased around September 2016 and February 2017 (Fig. 14c), when there were no harvesting events.

#### 5. Discussion

## 5.1. The requirements of remote sensing data to detect frequent alfalfa harvests

The typical size (width and length) of an alfalfa field is several hundred meters to 1.6 km (1 mile) in the SGP. Coarse spatial resolution remote sensing data may suffer from mixed pixel issues, limiting its ability to detect alfalfa harvesting events at a field scale. For example, here the MODIS pixel of  $\sim\!500$  m resolution included a portion of Bermuda pasture (Fig. 1). This mixed pixel might have caused lower sensitivities of VIs to alfalfa harvests as compared to finer spatial resolution datasets (Landsat and Sentinel-2) (Fig. 13). Thus, spatial resolutions of 100 m or finer, depending on the sizes of the fields, are needed for monitoring field-scale alfalfa harvests in this region.

Alfalfa is harvested multiple times during a year and vegetation can regrow quickly, depending on growth stage and water availability. Tracking of frequent harvesting events requires high temporal resolution remote sensing data. However, most fine resolution satellite remote sensing products have relatively low temporal resolutions. Both Landast-7 and -8 have a temporal resolution of 16-days. Combining them together results in an improved temporal resolution of 8-days. However, not all Landsat-7 and -8 images were effective observations as they were affected by adverse weather conditions. As a result, even the combined Landsat data were not temporally high enough to track all alfalfa harvesting events (Fig. 5 middle panel). Although Sentinel-2 has a 5-day temporal resolution, it still missed the first harvesting event in 2017 (Fig. 6 middle panel). One possible reason is that Sentinel-2B was launched on March 7, 2017. Before the launch of Sentinel-2B, Sentinel-2 mission's temporal resolution was only 10-days due to just one satellite (Sentinel-2A) being in orbit. Effective fine spatial resolution observation (i.e., cloud and cloud shadow free) at a higher temporal resolution (i.e., at least an 8-day interval) is necessary to adequately characterize the

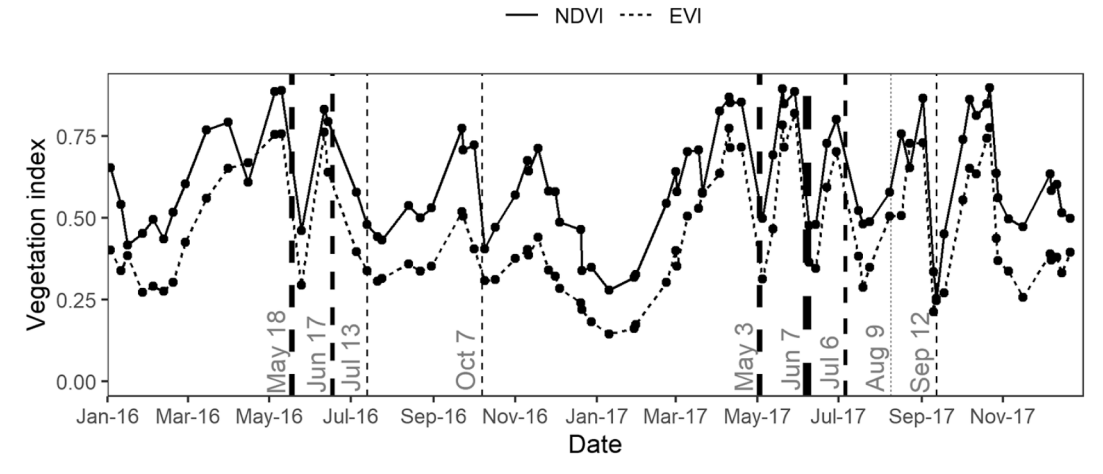


Fig. 9. Dynamic of NDVI and EVI after fusion of Landsat and Sentinel-2 data.

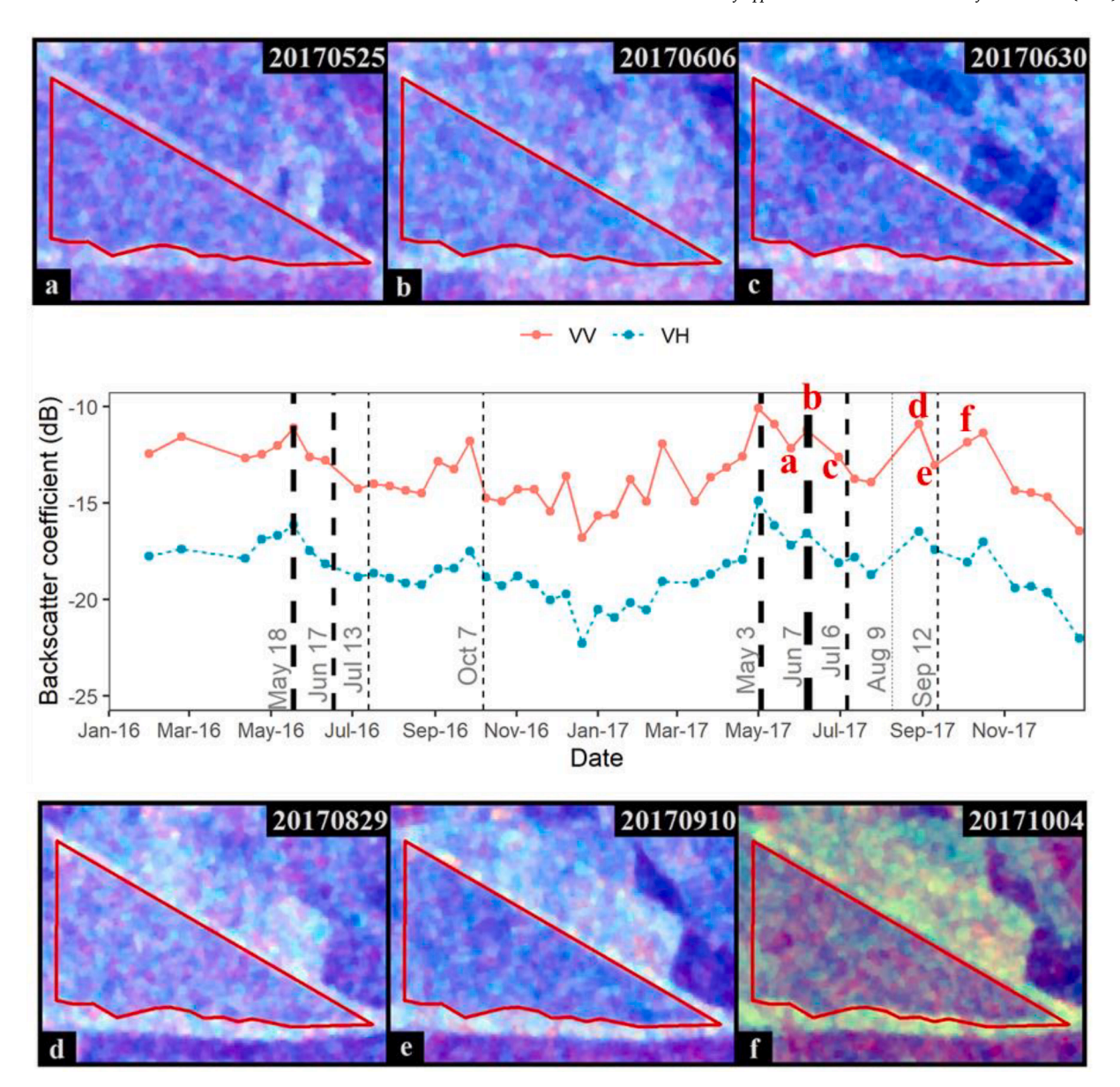


Fig. 10. Dynamics of VV (vertical transmit and vertical receive) and VH (vertical transmit and horizontal receive) backscatter coefficient (dB) from Sentinel-1 in orbit 34 and color composite (VV, VH, and VV/VH) images for large and small harvesting events in 2017.

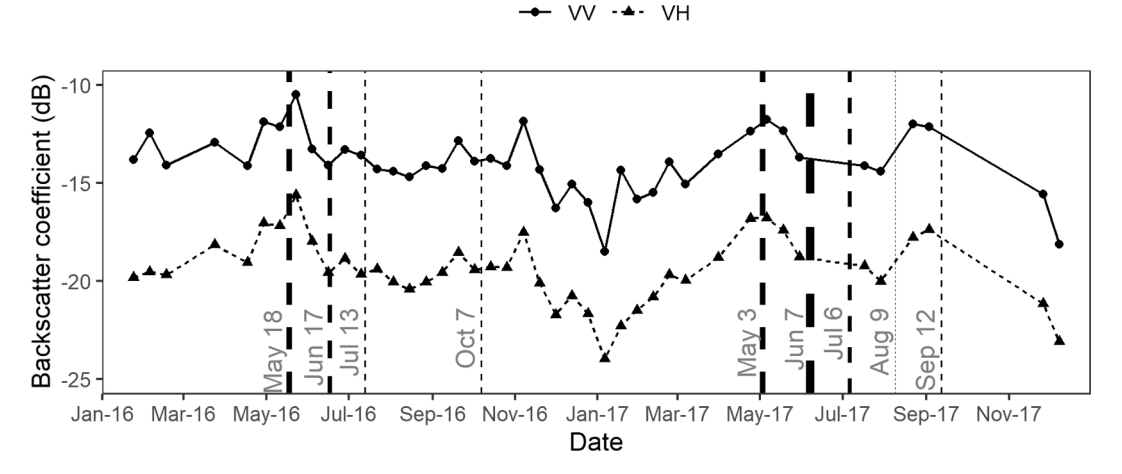


Fig. 11. Dynamics of VV and VH backscatter coefficient (dB) from Sentinel-1 in orbit 107.

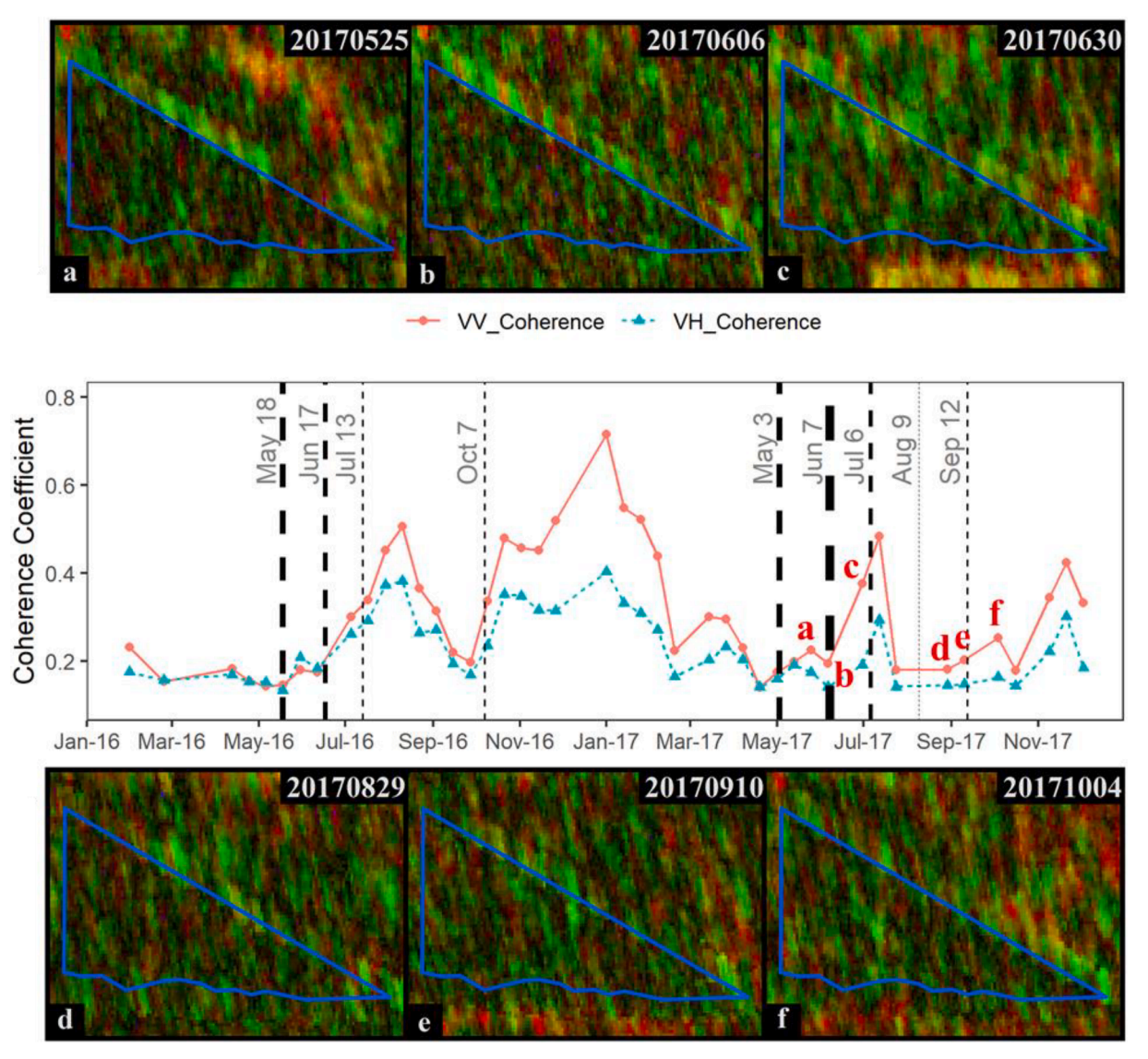


Fig. 12. Dynamics of VV and VH interferometric coherence coefficient from Sentinel-1 in orbit 34 and color composite (VV, VH, and VV/VH) images for large and small harvesting events.

localized disturbances/management practices such as frequent harvesting of alfalfa in this study.

#### 5.2. Data fusion to increase temporal resolution

Using data fusion approaches to increase temporal resolution is necessary to meet the requirements of both spatial and temporal resolutions for detecting alfalfa harvests. The HLS dataset harmonizes the Landsat-8 and Sentinel-2 data together through radiometric and geometric corrections to increase the temporal resolution to facilitate timeseries analysis. Our results showed that HLS (Fig. 7) greatly increased the number of available observations compared to any single fine spatial resolution dataset (Figs. 5 and 6 middle panels). However, the noise level was high in HLS-derived VIs (Figs. 7 and 13d). The direct comparison between HLS-derived VIs with those directly from Landsat (Fig. S1) and Sentinel-2 (Fig. S2) showed that the noises were high in the harmonized time-series of HLS data. Further improvement of HLS and temporal compositing methods to reduce the noises in the harmonized time-series of HLS data is necessary to better facilitate its application in detecting alfalfa harvests at the regional scale.

In addition to the HLS dataset, we also combined Landsat (both 7 and 8) and Sentinel-2 imageries based on the NDVI values up to one week

apart (Fig. 8), and increased the temporal resolution of optical remote sensing data to detect frequent alfalfa harvests. The fused Landsat and Sentinel-2 VIs (Fig. 9) were more effective in detecting each harvesting event in comparison to any single dataset (Fig. 5and 6 middle panels). In addition, the noise level in our fused Landsat and Sentinel-2 dataset was lower than those in HLS (Fig. 7), suggesting that simple statistical transformation functions are also effective in fusing these two datasets at the site level. However, more rigid data fusion approaches, like HLS, is needed for regional scale analyses. These results demonstrate that merging fine spatial resolution datasets from different optical remote sensing sensors to increase temporal resolution is an effective way to better track the field scale management practices such as frequent alfalfa harvesting events.

An alternative approach is to fuse optical and radar data, which provides both spectral and structural information of land surfaces. For example, Zhou et al. (2017a) mapped winter wheat in an urban agricultural region in China using multi-temporal SAR (Sentinel-1A) and optical images (Landsat-8). Sentinel-1A and 2A were used for crop classification in Japan (Sonobe et al., 2017). However, there is a lack of framework and effective methods for integrating optical and radar data (Joshi et al., 2016).

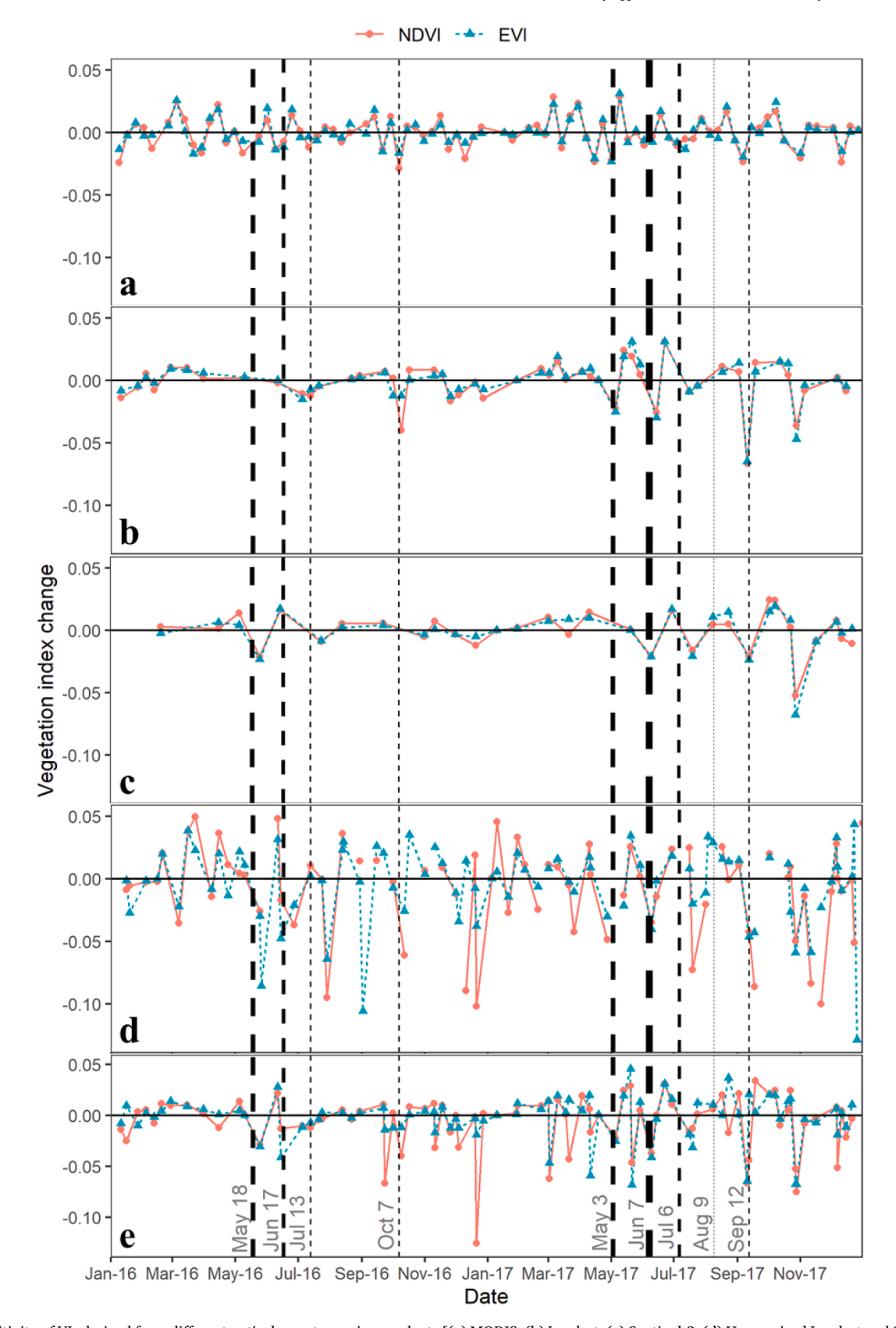


Fig. 13. Sensitivity of VIs derived from different optical remote sensing products [(a) MODIS, (b) Landsat, (c) Sentinel-2, (d) Harmonized Landsat and Sentinel-2, and (e) Fused Landsat and Sentinel-2.] to different sized harvesting events.

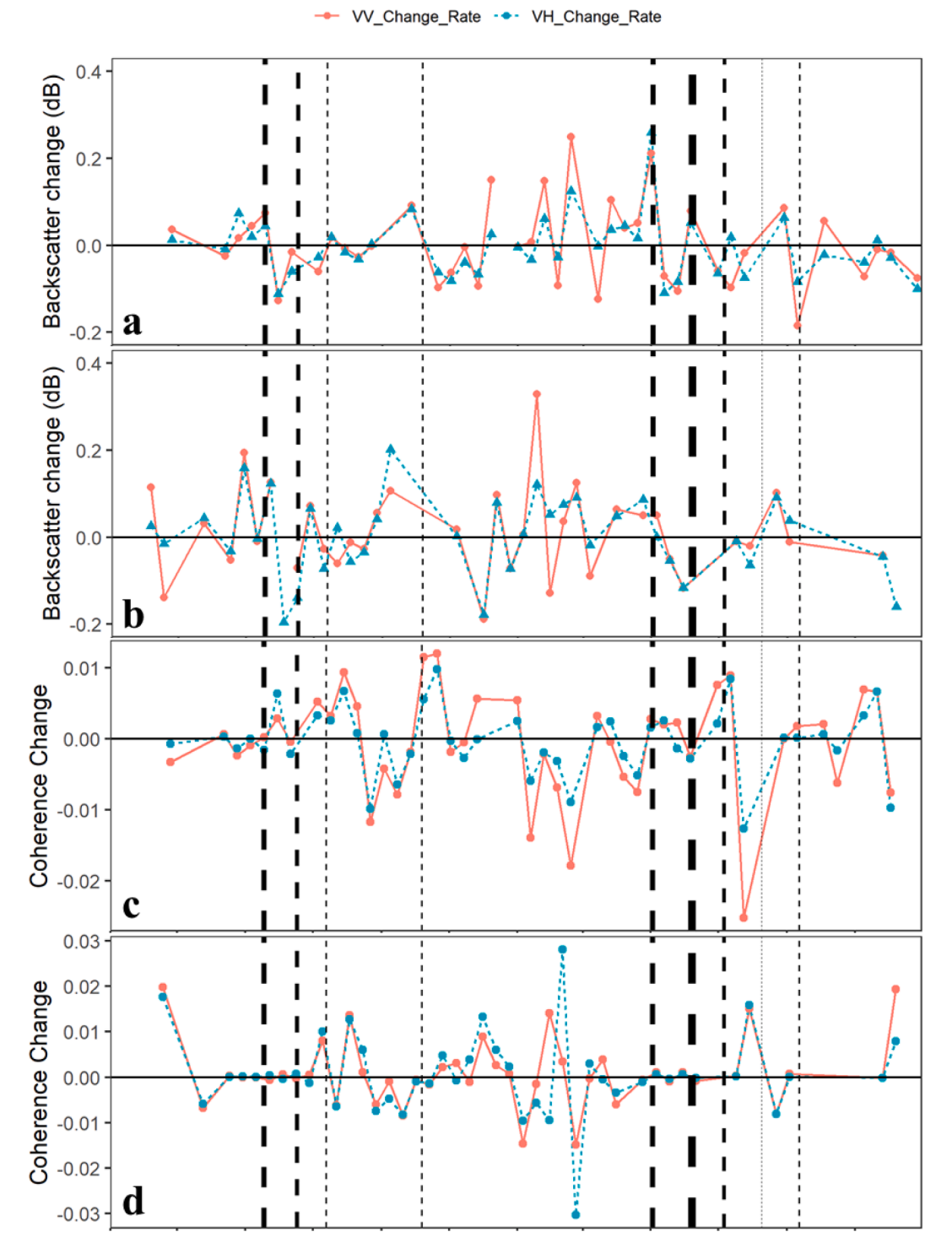


Fig. 14. Sensitivity of radar backscatters and interferometric coherence with small (a for backscatter and c for coherence) and large (b for backscatter and d for coherence) observation angles.

## 5.3. Passive optical remote sensing versus active radar in detecting frequent alfalfa harvests

Vegetation indices derived from optical remote sensing datasets have been widely used in vegetation monitoring (Zhang et al., 2006; Zhou et al., 2017b). However, there is always a tradeoff between spatial and temporal resolutions. Coarse spatial resolution data (e.g., MODIS) can have mixed pixel issues, while low temporal resolution data might miss the signal in high frequency and localized disturbances (e.g., frequent alfalfa harvests in this study). Moreover, passive optical remote sensing

is susceptible to adverse weather conditions.

Active radar can function in all weather conditions. Radar has been used in monitoring crop harvest patterns (Tamm et al., 2016; Zhao et al., 2014) and crop residues (Daughtry et al., 2005; McNairn et al., 2001). Radar sensors with high spatial and temporal resolutions provide an opportunity to analyze the response of time-series radar data to frequent alfalfa harvests. Our results indicated that Sentinel-1 (Fig. 6) had the potential to detect alfalfa harvests especially in observations with a small incident angle (34.31°). However, the visual aesthetics of radar signals were less intuitive than optical data. Additionally, other

compounding factors, including incident angle, size of harvesting, and soil moisture, need to be further examined.

#### 6. Conclusion

To assess the potential of different remote sensing datasets to detect frequent alfalfa harvests, active and passive remote sensing data of different spatial and temporal resolutions were used. Our results indicate that both fine spatial and high temporal resolutions are important to reliably detect frequent alfalfa harvests. Landsat and Sentinel-2 were more effective to detect alfalfa harvests compared to MODIS because of their finer spatial resolutions, which helped overcome the issue of a mixed pixel. However, they missed some harvesting events because of lower temporal resolutions. The HLS dataset that fused both Landsat-8 and Sentinel-2 data detected most of the harvesting events. However, the noise level in the HLS dataset was high. Thus, we fused Landsat (7 and 8) and Sentinel-2 data with a strict quality control to further increase the temporal resolution of effective optical remote sensing data. Our fused dataset performed better in detecting frequent alfalfa harvesting events than any single dataset, while also incurring less noise than the HLS dataset. Radar backscatter coefficients from Sentinel-1 were decreased by alfalfa harvests in the small incident angle observations (34.31°). In contrast, interferometric coherence coefficients were mostly increased by alfalfa harvests. Both backscatter and coherences values in the large incident angle observations did not show consistent responses to alfalfa harvesting events. Our results showed that active radar has the potential to detect alfalfa harvests. However, it is required to further investigate the impacts of incident angle, size of harvesting, and soil moisture on radar backscatter. Thus, fusing optical remote sensing datasets to increase temporal resolution is a more suitable approach to detect frequent alfalfa harvesting events at the current stage. This study demonstrates the potential of utilizing multiple remote sensing datasets to monitor field scale disturbances, including all types of hay harvesting (e.g., alfalfa, winter wheat, prairie grasslands).

#### **Declaration of Competing Interest**

The authors declare that they have no known competing financial interests or personal relationships that could have appeared to influence the work reported in this paper.

#### Acknowledgments

This study was supported in part by research grants from the National Science Foundation (NSF) EPSCoR (OIA-1946093) and the U.S. Geological Survey under Grant/Cooperative Agreement No. G18AP00077.

#### Appendix A. Supplementary data

Supplementary data to this article can be found online at https://doi.org/10.1016/j.jag.2021.102539.

#### References

- Bartsch, A., Widhalm, B., Leibman, M., Ermokhina, K., Kumpula, T., Skarin, A., Wilcox, E.J., Jones, B.M., Frost, G.V., Höfler, A., 2020. Feasibility of tundra vegetation height retrieval from Sentinel-1 and Sentinel-2 data. Remote Sens. Environ. 237, 111515.
- Bégué, A., Arvor, D., Bellon, B., Betbeder, J., De Abelleyra, D., Ferraz, R.P.D., Lebourgeois, V., Lelong, C., Simões, M., Verón, S.R., 2018. Remote sensing and cropping practices: A review. Remote Sens. 10, 99.
- Burris, W.R., 2001. Alfalfa for Beef Cattle. University of Kentucky.
- Butler, T.J., Biermacher, J.T., Interrante, S.M., Sledge, M.K., Hopkins, A.A., Bouton, J.H., 2012. Production and economics of grazing alfalfa in the Southern Great Plains. Crop Sci. 52, 1424–1429.

- Caddel, J., Stritzke, J., Berberet, R., Bolin, P., Huhnke, R., Johnson, G., Kizer, M., Lalman, D., Mulder, P., Waldner, D., Ward, C., Zhang, H., Cuperus, G., 2001. Alfalfa production guide for the southern Great Plains. http://pods.dasnr.okstate.edu/docushare/dsweb/Get/Document-8734/E-826.pdf (Accessed 13 August 2018).
- Claverie, M., Ju, J., Masek, J.G., Dungan, J.L., Vermote, E.F., Roger, J.-C., Skakun, S.V., Justice, C., 2018. The Harmonized Landsat and Sentinel-2 surface reflectance data set. Remote Sens. Environ. 219, 145–161.
- Daughtry, C.S.T., Hunt, E.R., Doraiswamy, P.C., McMurtrey, J.E., 2005. Remote Sensing the Spatial Distribution of Crop Residues. Agron. J. 97, 864–871.
- Flynn, K.C., Zhou, Y., Gowda, P.H., Moffet, C.A., Wagle, P., Kakani, V.G., 2020. Burning and Climate Interactions Determine Impacts of Grazing on Tallgrass Prairie Systems. Rangeland Ecol. Manage. 73, 104–118.
- Griffiths, P., Nendel, C., Hostert, P., 2019. Intra-annual reflectance composites from Sentinel-2 and Landsat for national-scale crop and land cover mapping. Remote Sens. Environ. 220, 135–151.
- Hosseini, M., McNairn, H., Merzouki, A., Pacheco, A., 2015. Estimation of Leaf Area Index (LAI) in corn and soybeans using multi-polarization C-and L-band radar data. Remote Sens. Environ. 170, 77–89.
- Huete, A., Didan, K., Miura, T., Rodriguez, E.P., Gao, X., Ferreira, L.G., 2002. Overview of the radiometric and biophysical performance of the MODIS vegetation indices. Remote Sens. Environ. 83, 195–213.
- Joshi, N., Baumann, M., Ehammer, A., Fensholt, R., Grogan, K., Hostert, P., Jepsen, M.,
   Kuemmerle, T., Meyfroidt, P., Mitchard, E., Reiche, J., Ryan, C., Waske, B., 2016.
   A Review of the Application of Optical and Radar Remote Sensing Data Fusion to
   Land Use Mapping and Monitoring, Remote Sens. 8, 70.
- Mandal, D., Kumar, V., Ratha, D., Lopez-Sanchez, J.M., Bhattacharya, A., McNairn, H., Rao, Y., Ramana, K., 2020. Assessment of rice growth conditions in a semi-arid region of India using the Generalized Radar Vegetation Index derived from RADARSAT-2 polarimetric SAR data. Remote Sens. Environ. 237, 111561.
- McNairn, H., Duguay, C., Boisvert, J., Huffman, E., Brisco, B., 2001. Defining the sensitivity of multi-frequency and multi-polarized radar backscatter to post-harvest crop residue. Can. J. Remote Sens. 27, 247–263.
- McNairn, H., Jiao, X., Pacheco, A., Sinha, A., Tan, W., Li, Y., 2018. Estimating canola phenology using synthetic aperture radar. Remote Sens. Environ. 219, 196–205.
- McPherson, R.A., Fiebrich, C.A., Crawford, K.C., Kilby, J.R., Grimsley, D.L., Martinez, J. E., Basara, J.B., Illston, B.G., Morris, D.A., Kloesel, K.A., 2007. Statewide monitoring of the mesoscale environment: A technical update on the Oklahoma Mesonet. J. Atmos. Oceanic Technol. 24, 301–321.
- Müller-Wilm, U., Devignot, O., Pessiot, L., 2016. Sen2Cor Configuration and User Manual. In: France. ESA.
- Noland, R.L., Wells, M.S., Coulter, J.A., Tiede, T., Baker, J.M., Martinson, K.L., Sheaffer, C.C., 2018. Estimating alfalfa yield and nutritive value using remote sensing and air temperature. Field Crops Res. 222, 189–196.
- Sonobe, R., Yamaya, Y., Tani, H., Wang, X., Kobayashi, N., Mochizuki, K.-I., 2017.
  Assessing the suitability of data from Sentinel-1A and 2A for crop classification.
  GIScience Remote Sens. 54, 918–938.
- Tamm, T., Zalite, K., Voormansik, K., Talgre, L., 2016. Relating Sentinel-1 interferometric coherence to mowing events on grasslands. Remote Sens. 8, 802.
- Tucker, C.J., 1979. Red and photographic infrared linear combinations for monitoring vegetation. Remote Sens. Environ. 8, 127–150.
- U.S. Department of Agriculture National Agricultural Statistics Services, 2019. Crop Production 2018 Summary. Available from https://www.nass.usda.gov/Publications/Todays\_Reports/reports/cropan19.pdf.
- Undersander, D., Cosgrove, D., Cullen, E., Rice, M.E., Renz, M., Sheaffer, C., Shewmaker, G., Sulc, M., 2011. Alfalfa Management Guide. American Society of Agronomy, Crop Science Society of America, and Soil Science Society of America.
- Weiss, M., Jacob, F., Duveiller, G., 2020. Remote sensing for agricultural applications: A meta-review. Remote Sens. Environ. 236, 111402.
- Yang, S., Feng, Q., Liang, T., Liu, B., Zhang, W., Xie, H., 2018. Modeling grassland above-ground biomass based on artificial neural network and remote sensing in the Three-River Headwaters Region. Remote Sens. Environ. 204, 448–455.
- Zhang, X., Friedl, M.A., Schaaf, C.B., 2006. Global vegetation phenology from Moderate Resolution Imaging Spectroradiometer (MODIS): Evaluation of global patterns and comparison with in situ measurements. *Journal of Geophysical Research*. Biogeosciences 1111.
- Zhao, L., Yang, J., Li, P., Zhang, L., 2014. Characteristics Analysis and Classification of Crop Harvest Patterns by Exploiting High-Frequency MultiPolarization SAR Data. IEEE J. Sel. Top. Appl. Earth Obs. Remote Sens. 7, 3773–3783.
- Zhou, T., Pan, J., Zhang, P., Wei, S., Han, T., 2017a. Mapping winter wheat with multi-temporal SAR and optical images in an urban agricultural region. Sensors 17, 1210.
- Zhou, Y., Gowda, P.H., Wagle, P., Ma, S., Neel, J.P., Kakani, V.G., Steiner, J.L., 2019. Climate effects on tallgrass prairie responses to continuous and rotational grazing. Agronomy 9, 219.
- Zhou, Y., Xiao, X., Wagle, P., Bajgain, R., Mahan, H., Basara, J.B., Dong, J., Qin, Y., Zhang, G., Luo, Y., Gowda, P.H., Neel, J.P.S., Starks, P.J., Steiner, J.L., 2017b. Examining the short-term impacts of diverse management practices on plant phenology and carbon fluxes of Old World bluestems pasture. Agric. For. Meteorol. 237–238, 60–70.
- Zhu, L., Walker, J.P., Tsang, L., Huang, H., Ye, N., Rüdiger, C., 2019. A multi-frequency framework for soil moisture retrieval from time series radar data. Remote Sens. Environ. 235, 111433.